Engineering and Technology Journal
Journal homepage: https://etj.uotechnology.edu.iq

Study the Growth of Apatite Layer on Biodegradable Glass as Bioactive Scaffolds

Zainab I. Dhary*, **Alaa A. Atiyah**, **Saad B. H. Farid**

Materials Engineering Dept, University of Technology-Iraq, Alsina'a Street, 10066 Baghdad, Iraq.
*Corresponding author Email: Zainab14.i.d@gmail.com

HIGHLIGHTS

- The maximum compressive strength of the bioglass scaffold was found to be about 5.6MPa.
- The prepared scaffold of bioglass has open porosity and interconnection ranging from about 75 to 78 %.
- The glass scaffolds can be considered promising for bone defects and replacement applications.

ARTICLE INFO

Handling editor: Akram R. Jabur
Keywords :

Bioglass 13-93
bioactivity
bone regeneration
Scaffold
Porosity

ABSTRACT

Bioglass offers a variety of uses for tissue engineering due to its good biocompatibility and chemical composition, similar to a mineral portion of the body. The synthesis of bioglass 13-93 scaffold was achieved by salt leaching technique, and potassium chloride (KCl) was used as porogen with particle sizes of (200-250) µm. Then, sintering to 750 ◦C for around 1 hour was performed. The resultant materials were examined by Fourier transform infrared spectroscopy (FTIR), X-ray diffraction (XRD), and scanning electron microscopy (SEM). They were immersed in a solution of simulated body fluids (SBF) for 7 and 14 days, respectively. Initially, calcium phosphate was created. After 7 and 14 days, the surface comprised of developed crystalline apatite. The bioactivity of scaffolds that were created and examined. The FTIR, SEM, and XRD experiments were done before and after immersion of the sample in SBF. The results showed that the scaffolds contained open and interconnected pores with porosities ranging between (75-78%). The maximum value of compressive strength of the prepared scaffold was about 5.6MPa. Based on the obtained results, the glass scaffolds can be considered promising for bone defects and replacement applications.

1. Introduction

Osteoinductive and osteoconductive filler components can repair constrained bone defects [1, 2]. Although no optimal biological answer currently exists for reconstituting architectural bone loss, including segmental defects within limbs. For the past several decades, several treatments have been employed to repair significant bone defects, like bone autografts, allografts, bone cement, and porous metals. Despite their benefits, however, several of these treatments have drawbacks such as availability, donor site morbidity, longevity, costs, and in-comfortable host bone healing. Thus, biocompatible implants are required to perform many functions that living bone does, such as morphology, strength, bioactivity, load-bearing capabilities, and porosity [3, 4].

A ceramic - scaffold is a significant component of tissue engineering in bone regeneration because it acts as a framework enabling cell interactions and the production of bone matrix components. The scaffolds act as osteoconductive moieties and promoters for creating a new center of bone formation. New bone is deposited as a creeping substitution of surrounding bone, and osteogenesis is the secondary mechanism by which new bone is generated [5, 6]. Bone regeneration scaffolds must meet and possess particular criteria and characteristics, such as the mechanical characteristics of the regenerative bone site, biocompatibility, biodegradability, and porosity [7, 8].

In vivo, polycaprolactone, poly (glycolic acid), collagen, and poly (lactic acid) scaffolds degrade and are replaced by a new bone matrix generated by tissue-forming cells [9, 10]. The materials' structural usage in bone healing has been difficult due to their low strength [11]. Because they are made of similar ions as a mineral component of bone, calcium phosphate

http://doi.org/10.30684/etj.2021.131678.1048
Received 26 September y 2021; Accepted 11 November 2021; Available online 17 July 2022
2412-0758/University of Technology-Iraq, Baghdad, Iraq

bioceramic like beta-tricalcium phosphate (β - TCP), bi-phasic calcium phosphate (BCP), and hydroxyapatite (HA) are practical bone repair materials. β -T C P scaffolds have become too weak to withstand the amount of physiologic loading, while synthesized HA degrades too slowly to allow osseous healing [12, 13].

Studies have focused mostly on glass compositions, including silicate 13-93 and 45S5 scaffold architectures with lower strength, such as human trabecular bone with compressive strengths ranging between (2-12) MPa [14–16]. These recent investigations have revealed that silicate 13-93 glass scaffolds manufactured using the salt leaching technique and a process that uses the solid freeform method have comparable compressive strengths to human cortical bones and an interconnected porous structure which is believed to aid bone infiltration [17- 19]. Strong porous bioglass scaffolds can potentially be beneficial implants in bone repair that have been loaded [20]. To increase the strength of the glass-ceramic scaffolds and glass sintering particles compressed with such freezing unidirectional, a pore-forming phase and salt leaching methods were employed [21,22]. Although it was possible to adjust the pore size and interconnectivity of a pore, it was challenging to manage the scaffold's responsibility to supply bone infiltration accurately.

There have been many previous studies that have evaluated the mechanical characteristics of the bioglass scaffolds in compression. Still, most have concentrated on creating or immersing in the simulated body fluids (SBF), a previously fabricated bioglass scaffold, to evaluate its elastic modulus and strength [23, 24]. Additional loading is added when loading, such as when long bones carry additional weight. Consequently, a complete study of the mechanical response of bioglass scaffolds for bone healing is required. The properties of the bioactive glass alter as it changes to hydroxyapatite (HA). Also extremely essential to the design for bioglass scaffolds in loaded bone regeneration are in vitro or in vivo environments for time-dependent mechanical responses [25, 26].

This research's objective was to manufacture porous scaffolds made from the bioglass 13-93 that had interconnected pores using the salt leaching technique. These scaffolds, which possessed the structure like human trabeculae bones, were utilized to evaluate the viability of bioglass as a suitable type for bone regeneration.

2. Experimental Work

2.1 Scaffold Production

The salt leaching technique was used to produce the bioglass 13-93 scaffold as follows:

1) To ensure complete dissolution, polyethylene glycol (PEG) is mixed with ethanol and then heated and stirred.
2) To decrease overall glass powder dispersing, the sieved bioglass 13-93 powder is continually mixed.
3) A proper amount of salts are added to the solution. Then, the solution is mixed for approximately 10–15 minutes.
4) Inside the Petri dish, material dispersion is moved around, covered, and protected by aluminum sheets.
5) An ethanol solvent was totally eliminated (approximately 1 day) through natural evaporation.
6) Once the sample has been immersed in distilled water for about seven days, the salt is completely dissolved. After that, water is refreshed every day to ensure the total dissolving of the salt.

2.2 Method to Generate Simulated Body Fluid (SBF)

To examine the degradation and bioactivity of the scaffolds, the S B F was exposed to static conditions. Reagent-grade compounds ($NaHCO_3$, NaCl, $K_2HPO_4{\bullet}3H_2O$, $MgCl_2{\bullet}6H_2O$, KCl, Na_2SO_4, and $CaCl_2$) were dissolved in water and buffered to a p H of 7.40 using tris (hydroxymethyl) amino - methane $(CH_2OH)_3 CNH_2$ and 1.0 M hydrochloric acid. For the conversion tests, 1 gram of powder in 100 ml and 1000 ml to SBF ratios were used. Glasses were placed in the polyethylene container with SBF solution and then maintained in a mixture incubated at 37°C for various amounts without being shaken. Before analysis, SBF powder was removed from de-ionized water and dried at around 60°C. A resistivity of around 18 MΩ-cm is employed during the testing [27]. Table 1 shows the solution of human blood plasma approximately the same as the ions concentration of SBF medium. As published previously, the HA-like layer was studied using XRD, SEM, and FTIR.

Table 1: The difference between human blood plasma and the solution of SBF [27].

	Concentration (mol/dm^3)	
Ion	**Simulated body fluid (SBF)**	**Human blood plasma**
Na^+	142.0	142.0
K^+	5.0	5.0
Mg^{2+}	1.5	1.5
Ca^{2+}	2.5	2.5
Cl^-	147.8	103.0
HCO^{3-}	4.2	27.0
HPO_4^{2-}	1.0	1.0
SO_4^{2-}	0.5	0.5

3. Characterizations

3.1 X-Ray Diffraction (XRD)

XRD analysis was used to analyze the various phases of the starting powders and a sintered scaffold. Inspecting was done at a rate of 5 °/min across a two-fold increased range of 10 ° - 90 ° using the X-ray and a Cu – K*a* radiation. It was determined that the JCPDS reference diffraction database could be used to identify the information.

3.2 Porosity Measurement

The pore-to-volume ratio within scaffolds, frequently called porosity, was estimated from the total volume of materials, including solid and non-solid pores, to a total non-solid volume. The scaffold's porosity was calculated from scaffold density and using the equations (1) [28].

$$P = 1 - \frac{m}{\rho_{polymer} \cdot v} \quad (1)$$

Where m the scaffold mass, **P** the scaffold porosity, **ρ** density of a polymer, and a scaffold volume are required.

3.3 Spectroscopy Analysis

The bioglass powder specimens were tested using a Bomem M B 100 analyzer and FTIR (Material Engineering/ Babylon University). In the case of IR examination, a 1 mg sample of a powder was mixed with 300 mg of KBr (infrared grade) and then placed on a pallet under vacuum to form a sample. Then the samples were scanned at a scan speed of 23 scans per minute while being exposed to light at a wavelength of 400–4000 cm^{-1}.

3.4 Microstructural Analysis

Ion sputter (E-1010, U K, Iran Polymer & Petrochemical Institute / Iran) was used to cover the scaffolds with gold before and after they were immersed in SBF. Dried scaffolds were first coated using gold before imaging with an SEM. Then, the voltage was raised to 12 kV to acquire the images.

3.5 Mechanical properties

To test these scaffolds in compression, the as-fabricated scaffold was put through the Instron test machine (Model 5881, Norwood, M A, U S A). A scaffold's compressive strength was evaluated when the crosshead moved at 0.5 mm/min and applied a 10 KN load. To evaluate the overall deformation, the crosshead was used to measure the motion of the sample. The contact area of the scaffold was ground with a surface grinder before the test (Chevalier Machinery I n c, Santa Fe Spring, USA).

4. Results and Discussion

The following measurements were taken to evaluate the porosity of bioglass 13-93 scaffolds utilizing Equation (1). In a highly porous bioglass 13-93 scaffold with open porosity and interconnected ranging from about 75 to 78 %. Better tissue growth and cell proliferation resulted from these studies, so an ideal was obtained. This is a notable success, supporting the theory that the bioglass 13-93 scaffolds have the potential to be suitable for bone tissue regeneration which falls within a range for human trabecular bones [8].

In Figure 1, it is strongly advised that the scaffolds be prepared before immersing in SBF as the previous scaffolds already possess a porous, uneven, somewhat rounded macro pores structure with a network of interconnected pores. Pores could be as large as 100 microns in diameter. Due to the applied porogen of the potassium chloride (KCl), the pore is produced in the salt leaching process. Therefore, the porosities and pore size of the scaffold created by the salt leaching procedure are controlled by particle size fixing and the amount of porogen used. The SEM photos showed bioglass 13-93 as a scaffold after being sintered at 750 ºC for one hour. The specimen described a non-uniform surface and interconnected pore, suggesting the occurrence of the dissociation mechanism and water penetration [29].

SEM pictures show that the broken portion of scaffolds following soaking into SBF for 7 days and 14 days produce contrasting images, as shown in Figure 2. The bioglass 13-93 surface structure changed due to the chemical reactions between a scaffold and the physiological fluid at the interface. After 7 days of immersing the bioglass in the SBF solution, the surface was entirely covered by homogeneous, visible, and small particles, as shown in Figure 2 (a and b). As the soaking period increased, the amount of developed apatite increased. A full layer of apatite covers a scaffold's whole pores during 14 days of incubation Figure 2b, c. According to many pieces of research, the mechanism for apatite generation in SBF was established by [30- 32]. This discovery was recently made public when it was stated that the production of apatite upon synthetic materials is prompted by functional compounds, which could show negative charges and then lead to amorphous calcium phosphate forming due to the resulting functional groups [33].

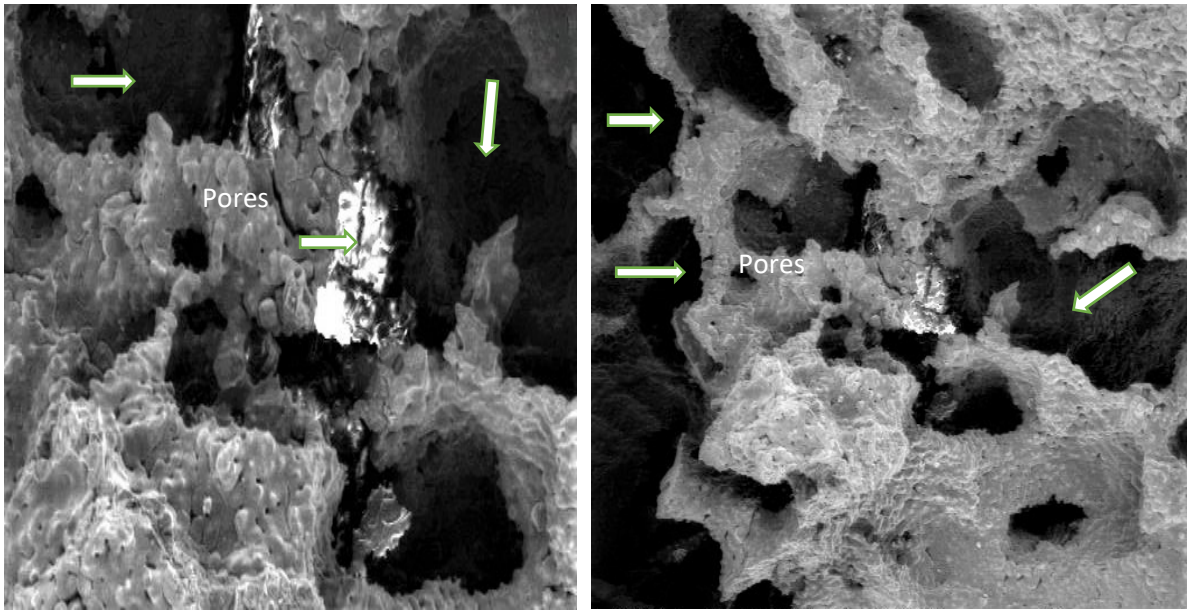

Figure 1: SEM showing pores of the bioglass 13-93 scaffolds before immersion in SBF

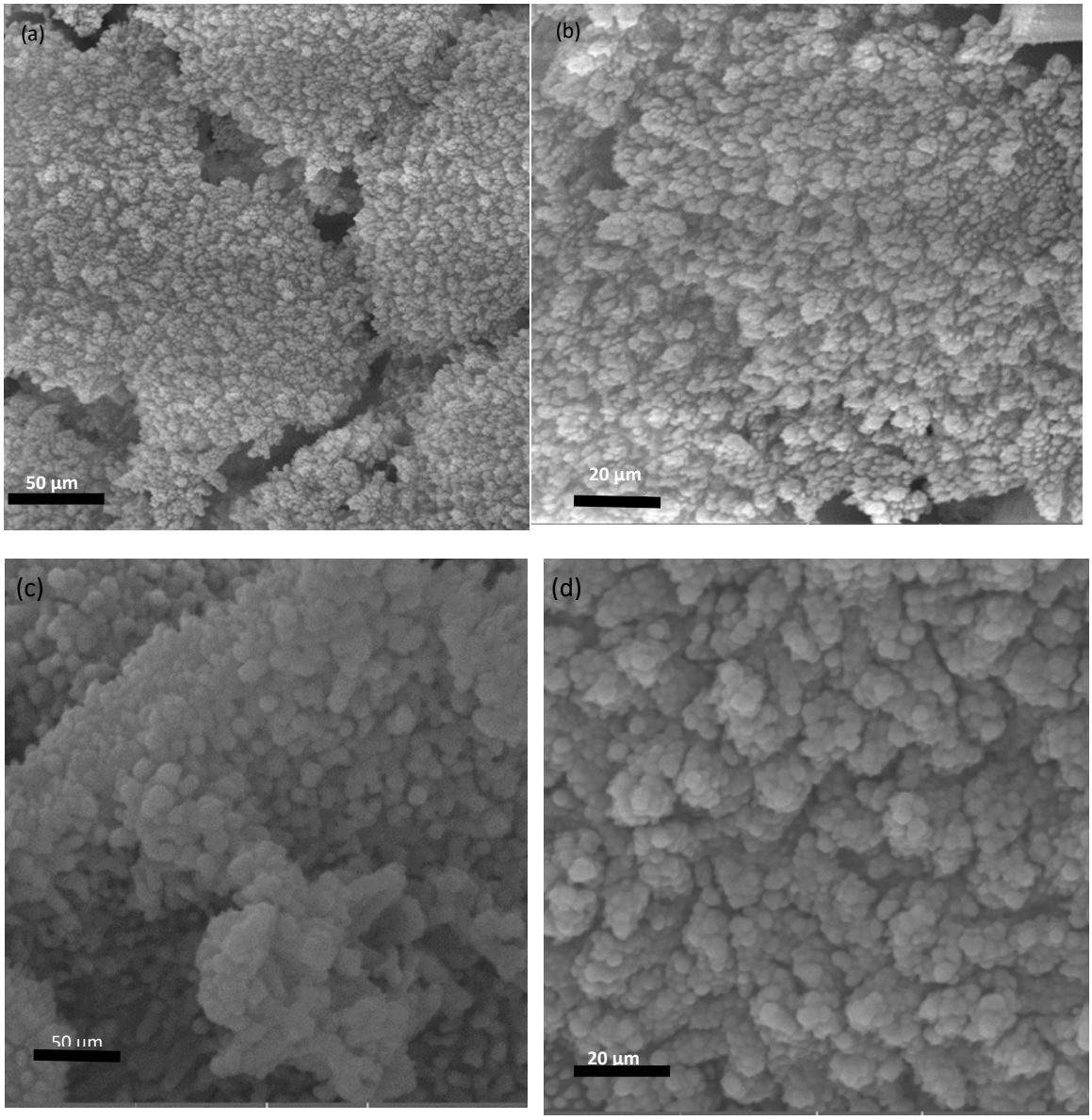

Figure 2: SEM photos of scaffolds after soaking in SBF for 7 days (a and b) and after 14 days (c &d) with different magnifications

Before and after immersion in SBF, a chemical analysis of bioglass 13-93 scaffolds are demonstrated in Figure 3 a, b, and c. When examined with an EDX analysis, bioglass 13-93 scaffold samples before immersion in S B F solution reveal the presence of four elements (Ca, O, Si, and P), as shown in (Figure 3a). In (Figure 3b, c), after immersion in SBF solution, the EDX test displayed that phosphorus and Calcium are the main constituents of a newly created layer. In addition, amorphous silica gels, formed during the apatite production process, were also found on a surface. Apatite formation begins with the interchange of calcium ions from the surface and solution, followed by the formation of silanol particles on the surface. This process is followed by the polymerization of silanol particles to generate amorphous silica gels. Finally, calcium and phosphate ions are transported to the surface, and apatite is formed. After 7 and 14 days of immersion in SBF, elemental analysis of a surface-displayed that the Ca / P ratio was approximately 1.65, similar to a 1.67 hydroxyapatite value. To confirm that a fluid circulation proved adequate to produce HA precipitation inside the 3D structure, HA crystals were detected in both the scaffold's pores and on the scaffold's surface. It is most likely that the existence of Si and Na is due to the glass on the underside of the particles. This is expected as X-ray has a large penetration [34].

The XRD graphs of a bioglass 13-93 scaffolds before and after immersion in SBF solutions for various time durations are shown in Figures 4 a, b, and c. Before immersing, the sample was glassy, exhibiting amorphous features Figure 4a. However, after immersing the bioglass scaffold in SBF over 7 days (Figure 4b), the HA phase was generated as evidenced by the development of 2 separate HA peaks around 26° (022), 28° (210), and 36° (211). In addition, other less visible peaks were found at 40° (310), 51° (213), and 63° (004). This proved the synthesized bioglass's biological activity. When the immersion duration was increased, the peak of the HA phase became sharper. This is attributed to the additional transformation of bioglass to HA Figure 4c [35].

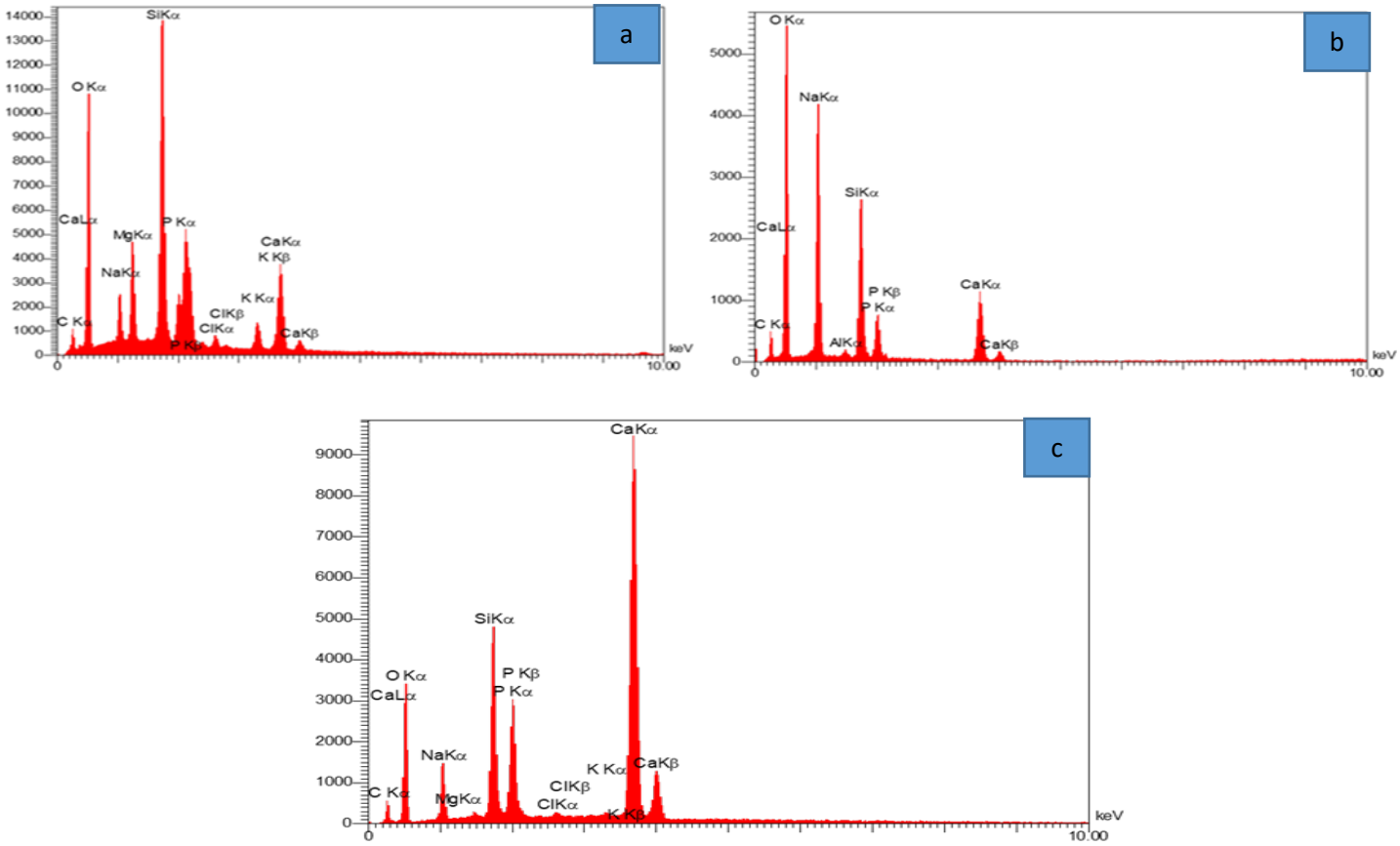

Figure 3: EDX analyses of bioglass 13-93 before (a) and after immersion in the SBF for (b) 7 and (c) 14 days.

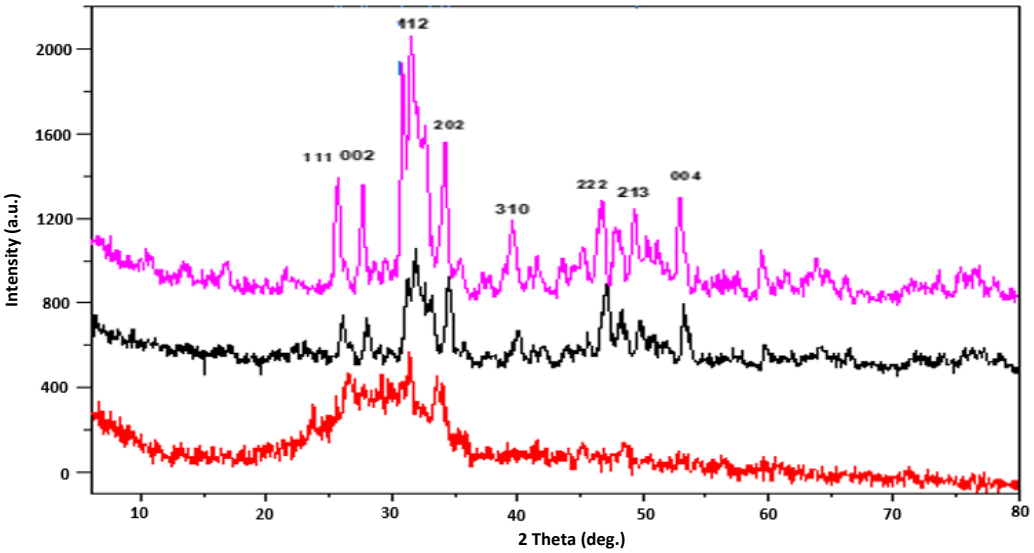

Figure 4: XRD spectrum of bioglass 13-93 scaffold before (a) and after soaking in the SBF for (b) 7 and (c) 14 days.

The FTIR spectra of the material before soaking in SBF for various periods are shown in Figure 5. The FTIR spectrum taken before soaking in SBF revealed the Si–O–Si stretch and bend bands. A vibration mode of an asymmetric stretch with Si–O–Si is visible around 1080 cm^{-1}, while a symmetric stretch with Si–O is visible around 449 cm^{-1}. The production of HA upon the surfaces of a specimen was noticed within the FTIR spectrum after being soaked in SBF at different times in SBF solution Figure 6. The development of two bands at 603 and 561 cm^{-1} was attributed to PO_4 bending vibrations, and a strong band around 1035 cm^{-1} was produced by PO_4 symmetrical stretching vibrations. Developing the HA layer weakened and eliminated the bands that were believed to be associated with Si–O–Si vibrational modes from bioglass [36].

Manufactured bioglass scaffolds were tested under compression to assess their stress/displacement response, as demonstrated above Figure 7. This stress is engineering stress calculated from the scaffold's initial cross-section area. Progressive cracking or compaction of a solid network of scaffolds could be responsible for the peaks and valleys in mechanical response [37]. Therefore, compressive strength for a scaffold was used as the high-value stress vs. displacement response. The results of this test suggest that the bioglass scaffold's highest mean compression strength has a value of 5.6 MPa, as demonstrated in the image below.

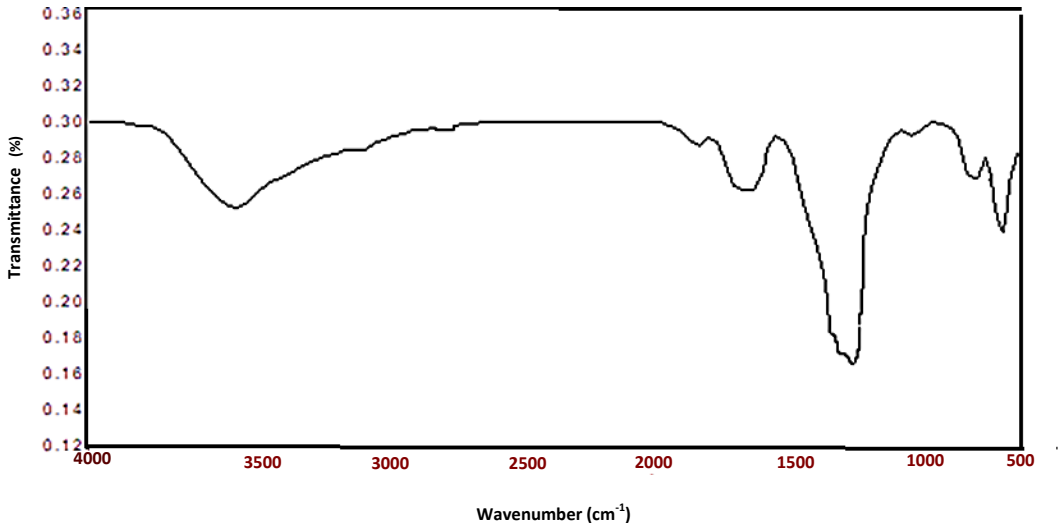

Figure 5: FTIR spectrum of the bioglass 13-93 scaffold.

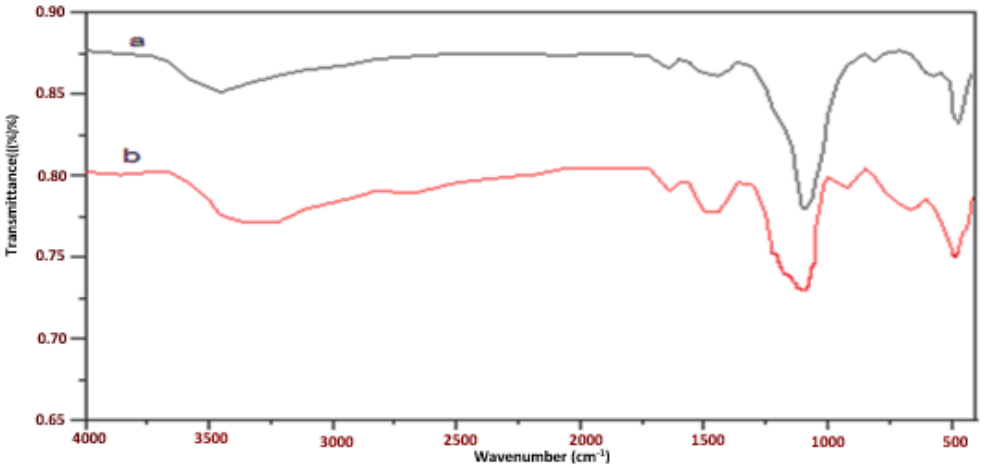

Figure 6: FTIR spectrum of the bioglass 13-93 scaffold after immersion in SBF (a) 7, and (b) 14 days

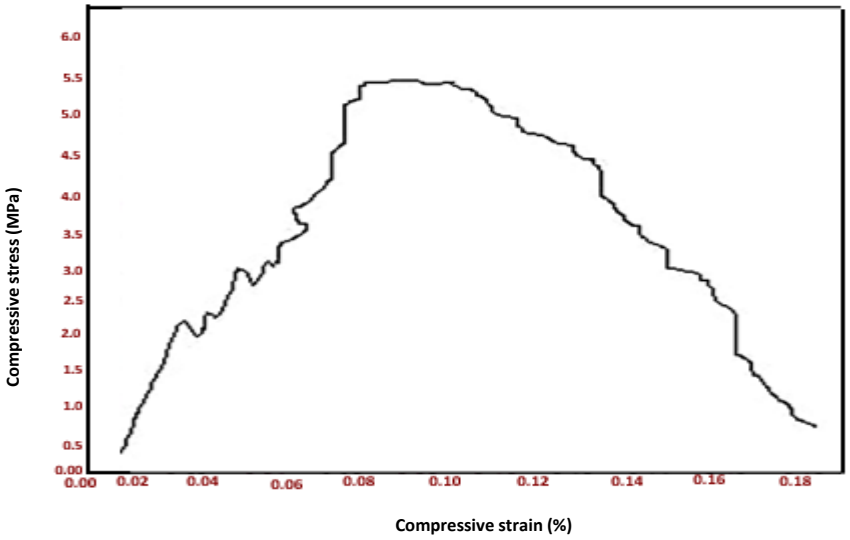

Figure 7: Compression stress vs. deformation for bioglass 13-93 scaffolds.

5. Conclusion

The experiment produced porous bioglass scaffolds with rapid degradation and biological activity. The salt leaching technique successfully produced the bioglass13–93 scaffold. An efficient technique for making bioglass used 13–93 glass precursors combined with PEG. After the heat - treatment at 750 °C for one hour, the scaffold stayed amorphous. The XRD test results indicate that all nitrates were stripped away at 750 °C. A fabricated glass scaffold product that contained bioglass 13–93 components has very good bioactivity in SBF. After 7 days and 14 days in S B F, the crystalline (Ca–P) layer formed, as shown by a divided P – O bending vibrational band at 500 to 600 cm^{-1}, which was validated by SEM, FTIR, and XRD investigations, confirming bioactivity of material necessary for uses in bone regeneration.

Author contribution

All authors contributed equally to this work.

Funding

This research received no specific grant from any funding agency in the public, commercial, or not-for-profit sectors.

Data availability statement

The data that support the findings of this study are available on request from the corresponding author.

Conflicts of interest

The authors declare that there is no conflict of interest.

References

[1] P. Giannoudis, H. Dinopoulos, E. Tsiridis, Bone substitutes: an update, Injury, 36S (2005) 20–37. https://doi.org/10.1016/j.injury.2005.07.029.

[2] C. Laurencin, Y. Khan, S. El-Amin, Bone graft substitutes, Expert Rev Med Devices, 3 (2006) 49–57. https://doi.org/10.1586/17434440.3.1.49

[3] L. Griffith LG, Polymeric biomaterials, Acta Mater, 48 (2000) 263–77. https://doi.org/10.1016/S1359-6454(99)00299-2

[4] M. grawal, B. Ray, Biodegradable polymer scaffolds for musculoskeletal tissue engineering, J Biomed Mater Res., 55 (2001) 141–50. https://doi.org/10.1002/1097-4636(200105)55:2%3C141::aid-jbm1000%3E3.0.co;2-j

[5] E. Groeneveld, J. Bergh, P. Holzmann, C. Bruggenkate, D. Tuinzing, and E Burger, Mineralization Processes in Demineralized Bone Matrix Grafts in Human Maxillary Sinus Floor Elevations, J. Biomed. Mater. Res. 48 (1999) 393–402. https://doi.org/10.1002/(sici)1097-4636(1999)48:4%3C393::aid-jbm1%3E3.0.co;2-c

[6] S Kadhum, S Salih, F Hashim, Preparation and characterization of polymer blend and nano composite materials based on PMMA used for bone tissue regeneration, Eng. Technol. J., 38 (2020) 501-509. https://doi.org/10.30684/etj.v38i4A.383

[7] P. Sepulveda, F. Ortega, M. Innocentini, V. Pandolfelli, Properties of Highly Porous Hydroxyapatite Obtained by the Gelcasting of Foams, J. Am. Ceram. Soc., 83 (2000) 3021–3024. http://dx.doi.org/10.1111/j.1151-2916.2000.tb01677.x

[8] J. Oleiwi, Q. Hamad, N. Kadhim, Study Compression, Hardness and Density properties of PMMA Reinforced by Natural Powder Used in Denture Base applications, Eng. Technol. J., 37 (2019) 522-527. https://doi.org/10.30684/etj.37.12A.5

[9] A. Goldstein, V. Patil, R. Moalli , Perspectives on tissue engineering of bone, Clin Orthop Rel Res., 357 (1999) 419–23. https://doi.org/10.1097/00003086-199910001-00041

[10] N. Collins MN, C. Birkinshaw, Hyaluronic acid based scaffolds for tissue engineering – a review, Carbohydr Polym., 92 (2013) 1262–1279. https://doi.org/10.1016/j.carbpol.2012.10.028

[11] U. Kneser, J. Schaefer, B. Munder, C. Klemt, C. Andree, B. Stark, Tissue engineering of bone, Minim Invasiv Ther. 11 (2022) 107–16. https://doi.org/10.3390/ma15031054

[12] L. Hench, Sol-Gel Synthesis of SiO2-CaO-Na2O-P2O5 Bioactive Glass Ceramic from Sodium Metasilicate, New j. glass ceram., 3 (2013) 1014-1017. https://doi.org/10.4236/njgc.2013.31003

[13] A. Mohammed, J. Oleiwi, E Al-Hassani, Influence of Nanocermic on Some Properties of Polyetheretherketone Based Biocomposites, Eng. Technol. J., 38 (2020) 1126-1136. https://doi.org/10.30684/etj.v38i8A.703

[14] C. Gerhardt, R. Boccaccini, Bioactive glass and glass-ceramic scaffolds for bone tissue engineering, Mater.,3 (2011) 3867–910. https://doi.org/10.3390/ma3073867

[15] F. Baino, C. Vitale-Brovarone, Three-dimensional glass-derived scaffolds for bone tissue engineering: current trends and forecasts for the future, J. Biomed. Mater. Res A., 97 (2011) 514–535. https://doi.org/10.1002/jbm.a.33072

[16] R Jones, Review of bioactive glass: from Hench to hybrids, Acta Biomater, 9 (2013) 4457–86. https://doi.org/10.1016/j.actbio.2012.08.023

[17] F. Baino, E. Verné, C.Brovarone, 3-D high strength glass-ceramic scaffolds containing fluoroapatite for load-bearing bone portions replacement, Mater. Sci. Eng: C.,29(2009)2055–2062. https://doi.org/10.1016/j.msec.2009.04.002

[18] X. Liu, N. Rahaman, Q. Fu, P. Tomsia , Porous and strong bioactive glass (13–93) scaffolds prepared by unidirectional freezing of camphene-based suspensions, Acta. Biomater., 8 (2012) 415–423. https://doi.org/10.1016/j.actbio.2011.07.034

[19] D. Doiphode, S .Huang, C. Leu, N. Rahaman, E. Day, Freeze extrusion fabrication of 13–93 bioactive glass scaffolds for bone repair, J. Mater. Sci: Mater. Med., 22 (2011) 515–23. https://doi.org/10.1007/s10856-011-4236-4

[20] S. Huang, D. Doiphode, N. Rahaman, C. Leu, S. Bal, E. Day, Porous and strong bioactive glass (13–93) scaffolds prepared by freeze extrusion fabrication, Acta Biomater.31 (2011) 415-423. https://doi.org/10.1016%2Fj.actbio.2011.07.034

[21] A. Deliormanli, A.N Rahaman, Direct-write assembly of silicate and borate bioactive glass scaffolds for bone repair, J. Eur. Ceram. Soc., 32 (2012) 3637–3646. https://doi.org/10.1016/j.jeurceramsoc.2012.05.005

[22] Q. Fu , E. Saiz , P. Tomsia, Bioinspired strong and highly porous glass scaffolds, Adv. Funct. Mater., 21 (2011) 1058–1063. https://doi.org/10.1002/adfm.201002030

[23] Q. Fu, E. Saiz, N .Rahaman, P. Tomsia, Bioactive glass scaffolds for bone tissue engineering: state of the art and future perspectives, Mater. Sci. Eng: C., 31 (2011) 1245–56. https://doi.org/10.1016/j.msec.2011.04.022

[24] A. Mehatlaf, A .Atiyah, S. Farid an Experimental Study of Porous Hydroxyapatite Scaffold Bioactivity in Biomedical Applications, Eng. Technol. J.,39 (2021) 977-985. https://doi.org/10.30684/etj.v39i6.2059

[25] Q. Fu, E. Saiz, P. Tomsia, Direct ink writing of highly porous and strong glass scaffolds for load-bearing bone defects repair and regeneration, Acta Biomater.,7 (2011) 3547–3554. https://doi.org/10.1016/j.actbio.2011.06.030

[26] Z. Al-Asadia, F .Al-Hasani, Effect of and Deposition on Biological Behavior of Ti-Base Alloys, Eng. Technol. J., 39 (2021) 573-585. https://doi.org/10.30684/etj.v39i4A.1906

[27] T. Kokubo and H. Takadama, How useful is SBF in predicting in vivo bone bioactivity?, Biomaterials., 27 (2006) 2907–2915. https://doi.org/10.1016/j.biomaterials.2006.01.017

[28] R Heijkants and T Van, polyurethane scaffold formation via a combination of salt leaching and thermally induced phase separation, J. Biomed. Mater. Res., 87 (2008) 921-32. https://doi.org/10.1002/jbm.a.31829

[29] H. Fu, Q .Fu , N. Zhou , W. Huang, M. Rahaman , D .Wang , X Liu, In vitro evaluation of borate-based bioactive glass scaffolds prepared by a polymer foam replication method', Mater. Sci. Eng., 29 (2009) 2275–228. https://doi.org/10.1016/j.msec.2009.05.013

[30] A. Davidson, A .Popa, M. Giazzon, M. Liley, L. Ploux, The interaction of cells and bacteria with surfaces structured at the nanometre scale, Acta Biomaterial., 6 92010) 3824–3846. https://doi.org/10.1016/j.actbio.2010.04.001

[31] S. Kenny and M. Buggy, Bone cements and fillers: a review, J. of Mat. Sci., 14 (2003) 923-938. doi: https://doi.org/10.1023/A:1026394530192.

[32] S. Mandel, and A. Tas, Brushite (CaHPO4·2H2O) to octacalcium phosphate (Ca8 (HPO4)2(PO4)4·5H2O) transformation in DMEM solutions, Mater. Sci. Eng. C., 30 (2010) 245–254. https://doi.org/10.1016/j.msec.2009.10.009

[33] R. Horváthová, L. Müller, A. Helebrant and F. Müller, In vitro transformation of OCP into Carbonated HA under physiological conditions, Mater. Sci. Eng:C.,28 (2008) 1414– 1419. https://doi.org/10.1016/j.msec.2008.03.010

[34] Q. Fu , M .Rahaman, B. Bal, W Huang, D. Day, Preparation and bioactive characteristics of a porous 13-93 glass, and fabrication into the articulating surface of a proximal tibia, J. Biomed. Mater. Res.,82 (2007) 222-229. https://doi.org/10.1002/jbm.a.31156

[35] G. Luo, Y. Ma, X .Cui, L. Jiang, M. Wu, Y .Hu, Y. Luo, H. Pana, C .Ruan, 13-93 bioactive glass/alginate composite scaffolds 3D printed under mild conditions for bone regeneration, RSC Advances, 7 (2017) 11880. https://doi.org/10.1039/C6RA27669E

[36] J.Chena, L .Zengb, X .feng, C. Tianshun, L. Zheng, Preparation and characterization of bioactive glass tablets and evaluation of bioactivity and cytotoxicity in vitro, Bioact Mater, 3 (2017) 315-321. https://doi.org/10.1016/j.bioactmat.2017.11.004

[37] X. Liu, M Rahaman, G. Hilmasa, B. Balc, Mechanical properties of bioactive glass (13-93) scaffolds fabricated by robotic deposition for structural bone repair, Acta Biomaterialia., 9 (2013) 7025-7034. https://doi.org/10.1016/j.actbio.2013.02.026